# Magnetic gravity compensation

V. S. Nikolayev · D. Chatain · D. Beysens · G. Pichavant

Received: 21 October 2009 / Accepted: 18 June 2010

Abstract Magnetic gravity compensation in fluids is increasingly popular as a means to achieve low-gravity for physical and life sciences studies. We explain the basics of the magnetic gravity compensation and analyze its advantages and drawbacks. The main drawback is the spatial heterogeneity of the residual gravity field. We discuss its causes. Some new results concerning the heterogeneity estimation and measurement are presented. A review of the existing experimental installations and works involving the magnetic gravity compensation is given for both physical and life sciences.

**Keywords** Magnetic levitation · diamagnetic ·  $microgravity \cdot life sciences \cdot physical sciences \cdot fluid$ 

## 1 Introduction

The opportunities of space experimentation are rare and their waiting time is often very long. For this reason, other ways of achieving reduced gravity (or simulated reduced gravity) are often used as a replacement. Drop tower and parabolic flight experiments provide short time low-gravity conditions, 4-9 s (Bremen drop tower) and 25 s (ESA Zero-g aircraft). For experiments

Presented at the ELGRA Symposium, Bonn, 1-4/9/2009.

V. S. Nikolayev  $\cdot$  D. Chatain  $\cdot$  D. Beysens  $\cdot$  G. Pichavant ESEME, Service des Basses Températures, CEA-Grenoble/DSM/INAC, 17 rue des Martyrs, 38054, Grenoble Cedex 9, France

V. S. Nikolayev · D. Beysens ESEME, PMMH-ESPCI-P6-P7, 10, rue Vauquelin, 75231 Paris Cedex 5, France E-mail: vadim.nikolayev@espci.fr - Possibility of controlling gravity levels (such as corresponding to the Moon, Mars etc.). - Possibility of controlling time variation of gravity, which can reproduce the acceleration (or decelera-

However, drawbacks and important limitations do exist. They will be discussed below. Some additional expla-

nations and definitions need to be given first.

1.1 Magnetic gravity compensation versus magnetic levitation

Magnetic gravity compensation means (total or partial) controlled reduction of the gravity force at each point

that require several minutes of low gravity, sounding rockets are available (ESA Maxus program, 13 min). For experiments that require long low-gravity duration as e.g. in life sciences, simulation devices like random positioning machines or clinostats can be used. However, all those means are prohibited in some cases because of security considerations. This concerns the flight experiments with highly flammable fluids like hydrogen and especially oxygen whose study is extremely important as they are the fuel components for space propulsion engines.

Another means is used more and more often to achieve long-time low gravity conditions: the magnetic gravity compensation. Comparing to the other approaches, this means has several undeniable advantages.

- It is performed in a ground-based facility with no moving parts so that a good security level can be achieved.
- The low gravity duration is unlimited.
- In principle, no waiting time.
- Reasonable cost.
- tion) of space vehicles.

of the object. This definition is not equivalent to that of magnetic levitation. The latter requires that the object be suspended, which does not necessarily means that the gravity is compensated *inside* the object when it is rigid. An example of levitation without gravity compensation is a transparent bowl placed on a superconductive disk. The bowl contains water with a gold-fish. The whole system is levitated. The photo by Ball (1990) shows that the meniscus of the water is flat, which means that both water and fish still experience the strong gravity. In what follows, the magnetic gravity compensation inside *fluids* will be considered. The term magnetic levitation will be rather applied to solid objects.

#### 1.2 Magnetic field and magnetic forces

The magnetic field is characterized by two variables, the magnetic field intensity  $\mathbf{H}$  [A/m] and the magnetic induction (called also magnetic flux density)  $\mathbf{B}$  [T]. In vacuum, they are related to each other by the expression

$$\mathbf{B} = \mu_0 \mathbf{H},\tag{1}$$

where  $\mu_0 = 4\pi \cdot 10^{-7}$  [T·m/A] is a constant called vacuum permeability.

The action of the magnetic field **H** on the matter provokes its own magnetic field called magnetization:

$$\mathbf{M} = \chi \mathbf{H},\tag{2}$$

where the coefficient of proportionality  $\chi$  is the magnetic susceptibility of the matter. The total magnetic field is equal to the sum of the external and induced fields,

$$\mathbf{B} = \mu_0(\mathbf{H} + \mathbf{M}) = \mu \mu_0 \mathbf{H},\tag{3}$$

where  $\mu=1+\chi$  is the magnetic permeability. The susceptibility defines the magnetic properties of the matter. When its absolute value is comparable or larger than unity, the matter is strongly magnetic. This is the case of ferromagnetic  $(\chi\gg 1)$  or superconductive  $(\chi\approx -1)$  substances. In what follows we will consider only weakly magnetic substances  $(|\chi|\ll 1)$  that can be either diamagnetic  $(\chi<0)$  or paramagnetic  $(\chi>0)$ .

It is important to note that for weakly magnetic substances,  $\chi \propto \rho$ , where  $\rho$  is the mass density. We will introduce the specific magnetic susceptibility,

$$\alpha = \chi/\rho,\tag{4}$$

which characterizes such substances.

Since  $\mu \approx 1$  with high accuracy for weakly magnetic substances such as air, the magnetic field created by a given installation in air is equal to that created in

vacuum. For this reason, the  $\mathbf{H}$  value is related to  $\mathbf{B}$  by the universal relation (1) and  $\mathbf{B}$  is also often called magnetic field.

Most pure fluids (e.g.  $H_2O$ ,  $H_2$ ,  $N_2$ ) and organic substances are diamagnetic. Some fluids (e.g.  $O_2$ , NO) are paramagnetic. The magnetic susceptibility of paramagnetic substances varies with temperature; that of diamagnetic substances is almost independent on temperature.

The magnetic force that acts on the unit volume of a substance is

$$\mathbf{F}_m = \frac{\chi}{2\mu_0} \nabla(\mathbf{B}^2),\tag{5}$$

where  $\nabla$  is the vector gradient operator. The gravity force per unit volume is

$$\mathbf{F}_q = \rho \mathbf{g},\tag{6}$$

where  $\mathbf{g}$  is the Earth gravity acceleration. An ideal compensation is achieved when

$$\mathbf{F}_m + \mathbf{F}_g = 0. \tag{7}$$

In a cylindrical r-z reference system where the z axis is directed upwards, this expression is equivalent to two equations,

$$\frac{\partial(B^2)}{\partial r} = 0 \tag{8}$$

$$\frac{\partial (B^2)}{\partial z} \equiv \nabla (B^2)_z = \frac{2\mu_0 g}{\alpha} \equiv G,\tag{9}$$

where  $\alpha$  is defined by (4). It means that for ideal compensation, the magnetic field would need to satisfy the equation  $B = \sqrt{c + Gz}$ , where c is an arbitrary constant. It has been shown by Quettier et al. (2005) that such a solution of the Maxwell equations for magnetic field does not exist so that the ideal compensation in any finite volume is impossible. In practice, the ideal compensation is achieved in a single or at most several points.

The stability of levitation is an important issue and is discussed by many authors starting from Braunbek (1939). For the purposes of the present study, it is important to mention that the levitation of a drop (or, generally, of a denser phase) in the surrounding gas is stable for diamagnetic fluids and unstable for paramagnetic fluids. On the contrary, the levitation of a bubble (or, generally, of a less dense phase) inside the liquid is stable for paramagnetic and unstable for diamagnetic fluids (Pichavant et al. 2009b).

#### 1.3 Required magnetic fields

It is important to underline that the magnetic compensation does not work for all substances at the same time.

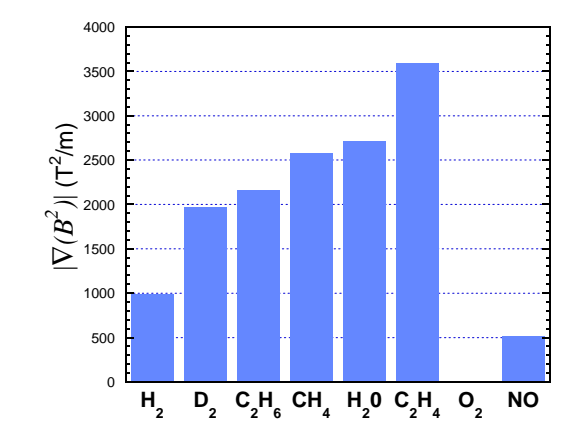


Fig. 1 The values of  $|\nabla(B^2)|$  required for gravity compensation for different fluids. The value for  $O_2$  is about 8  $T^2/m$ , which is so small that the corresponding bar is almost invisible. The signs of the required  $\nabla(B^2)_z$  are opposite for paramagnetic ( $O_2$  and  $O_2$ ) and diamagnetic (all other) fluids.

The  $\nabla(B^2)_z$  value required to compensate the gravity for a particular substance is given by the material constant G from Eq. 9. This value for different substances is shown in Fig. 1. Note that the G value for oxygen is the smallest. In most installations, the magnetic field is created with one or several co-axial solenoids, for which the radial component of the magnetic force is zero at the axis so that  $|\nabla(B^2)| = |\nabla(B^2)_z|$ , where  $\nabla(B^2)_z$  can be positive or negative. For this reason, one speaks often of  $|\nabla(B^2)|$  instead of  $\nabla(B^2)_z$ . Generally speaking, if a sample is submitted to  $\nabla(B^2)_z$  needed to compensate the gravity in a given substance, the gravity is not compensated for the others.

Note that Eq. 9 does not involve the density nor the mass of the sample. It means that the gravity will be compensated independently of the sample mass. If the gravity is compensated for the liquid phase of a substance, it is also compensated for the gas phase of the same substance, i.e. the buoyancy force for the gas bubbles or solid crystals in the liquid is compensated either.

In agreement with Eq. 9, the ability of a given magnetic installation to compensate the gravity is characterized by  $|\nabla(B^2)|$  that the installation is able to generate. The variation of this value along the axis of a typical solenoid (Fig. 2) shows that it has two extrema situated near the ends of the solenoid. These extrema are the most suitable places for the gravity compensation because they provide the maximum value of  $|\nabla(B^2)|$  for a given current in the solenoid. The upper extremum is a minimum and is suitable for the levitation of diamagnetic substances. The lower extremum is a maximum and is suitable for paramagnetic substances (Fig. 2).

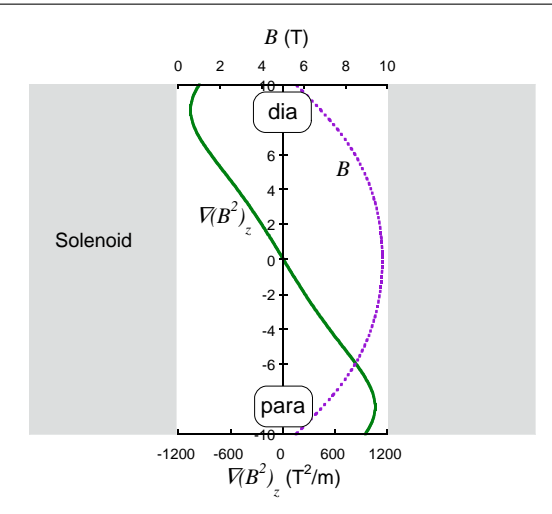


Fig. 2 An example of the variation of B and  $\nabla (B^2)_z$  along the axis z of a solenoid. The locations appropriate for levitation of dia- and para-magnetic samples are indicated. The HYLDE solenoid (Chatain and Nikolayev 2002) data are shown. z is measured in cm.

# 2 Past and present of magnetic gravity compensation

The bases of magnetic levitation have been put forward by Braunbek (1939). He has succeeded the levitation of diamagnetic bismuth that has a very low required  $|\nabla(B^2)|$ . He also provided the theory of levitation.

The first gravity compensation experiments have been realized in the 1960's independently in Berkeley (USA) by Lyon et al. (1965) and in Kharkov (USSR, Ukraine at present) by Kirichenko and Verkin (1968). They dealt with the studies of the boiling heat transfer in oxygen that had a very small required  $|\nabla(B^2)|$ . The magnetic field was created with resistive solenoids. These studies have been motivated by the importance of oxygen as a rocket fuel.

The development of superconductive solenoids opened the way to their wide use for gravity compensation. It has been pioneered by Beaugnon and Tournier (1991), who levitated multiple organic samples, both solid and fluid. The levitation of the frog embryos by Valles Jr et al. (1997) is the first known to us application of the magnetic gravity compensation in the life sciences. A large number of works on magnetic gravity compensation has been published since then. The known to us experimental installations available at present for magnetic gravity compensation are presented in Table 1 with their main parameters such as the maximum attainable  $|\nabla(B^2)|$  value and the bore diameter. The latter defines the maximum sample size that can be used. Installations that can attain  $\sim 3000 \text{ T}^2/\text{m}$  may be used for gravity compensation in water or biological tissues that consist mainly of water (cf. Fig. 1); their

 ${\bf Table} \ {\bf 1} \ \ {\bf Available} \ {\bf magnetic} \ {\bf gravity} \ {\bf compensation} \ {\bf installations} \ {\bf worldwide}$ 

Location	B, T	$ \nabla (B^2) , T^2/m$	Bore Ø, mm	Latest citation
Nottingham, UK	16.5	2940	50	Hill and Eaves (2008)
Nijmegen, NL	$\sim 17$	$\sim 3000$	40	Simon and Geim (2000)
Gainesville FL, USA	15	3000	66	Liu et al. (2010)
		760	195	Brooks and Cothern (2001)
Providence RI, USA	9.5	3200	11	Guevorkian and Valles (2004)
Xi'an, China	16.12	3026	51	Lu et al. (2008)
Hiroshima, Japan	15	$\sim 3000$	50	Sueda et al. (2007)
Tohoku, Japan		$\sim 4000$	52	Watanabe et al. (2003)
Tsukuba, Japan	8.5	448	50	Kiyoshi and Wada (2003)
	17	1600		,
Grenoble, France	10	1000	50	Nikolayev et al. (2006)
	2	10	180	Pichavant et al. (2009b)

bore diameters correspond to the thermally insulated part of the bore at room temperature. Two last lines in the table refer to the installations developed in our group, the HYdrogen Levitation DEvice (HYLDE) and Oxygen Low Gravity Apparatus (OLGA), respectively.

The physical sciences studies performed with the magnetic gravity compensation in fluids concerned mostly the shape and motion of bubbles and drops. The studies performed at isothermal conditions dealt with the drop shape (Tagami et al. 1999; Wunenburger et al. 2000; Sueda et al. 2007; Hill and Eaves 2008), drop vibrations (Beaugnon and Tournier 1991; Whitaker et al. 1998), drop coalescence (Beaugnon and Tournier 1991; Weilert et al. 1996), applications in microfluidics (Lyuksyutov et al. 2004), surface instability in the magnetic field (Catherall et al. 2003), and, more recently, a study of the liquid meniscus under fast acceleration change (Pichavant et al. 2009a, 2010). The non-isothermal studies concerned boiling (Lyon et al. 1965; Kirichenko and Verkin 1968; Nikolayev et al. 2006; Pichavant et al. 2009b), drop behavior under temperature gradients (Watanabe et al. 2003; Beysens et al. 2009), phase transitions under vibrations (Beysens et al. 2005a,b, 2007, 2008) and gravity influence on flame (Khaldi et al. 2010)

The life sciences studies are concerned with the microgravity influence on protein crystals' growth (Matsumoto et al. 2004; Lu et al. 2008), expression of genes (Babbick et al. 2007; Coleman et al. 2007; Manzano et al. 2009b), growth of living cells (Guevorkian and Valles 2004; Manzano et al. 2009c; Moes et al. 2009; Hammer et al. 2009) or example levitation of small creatures (Valles Jr et al. 1997; Liu et al. 2010), and plant morphology (Manzano et al. 2009a).

## 3 Magnetic force heterogeneity issue

It has already been mentioned that the ideal compensation is achieved only in isolated points. However, it is

possible to approach the ideal compensation conditions within a given accuracy in any volume. The effective gravity spatial heterogeneity is thus the most important issue that limits the applicability of magnetic gravity compensation.

The compensation quality can be characterized by the spatial distribution of the effective gravity acceleration

$$\mathbf{a}_{eff} = (\mathbf{F}_m + \mathbf{F}_g)/\rho = \mathbf{g} + \frac{\alpha}{2\mu_0} \nabla(\mathbf{B}^2)$$
 (10)

defined with (5,6). In practice, the non-dimensional acceleration heterogeneity  $\varepsilon = \mathbf{a}_{eff}/g$  is more convenient.

There are several possible causes for  $\mathbf{a}_{eff}$  spatial variation. Those related to the spatial variation of  $\nabla(B^2)$ manifest itself even in a single-component system, i.e. in a pure fluid sample where its gas and liquid phases might coexist. Additional spatial variation of the effective gravity appears in multi-phase samples where  $\alpha$ varies. This variation might lead to internal mechanical stresses or even component displacement in such systems and needs to be analyzed separately for each specific case, for which the magnetic susceptibility  $\chi$  for each of the components needs to be known with precision. Note that the magnetic susceptibility is well studied for life sciences systems for high frequency magnetic field. However,  $\chi$  value for the *constant* field might be very different and is yet to be determined experimentally. In the rest of this section we consider only the single-component fluids.

A spatial variation of  $\nabla(B^2)$  may appear in such fluids because of several reasons. First, there is a variation of the background force field of the magnetic installation (sec. 3.1). Second, distortions can be induced by the sample. These include the variation because of the experimental cell structure (see below) and the fluid itself. Let us consider each of the heterogeneity causes separately.

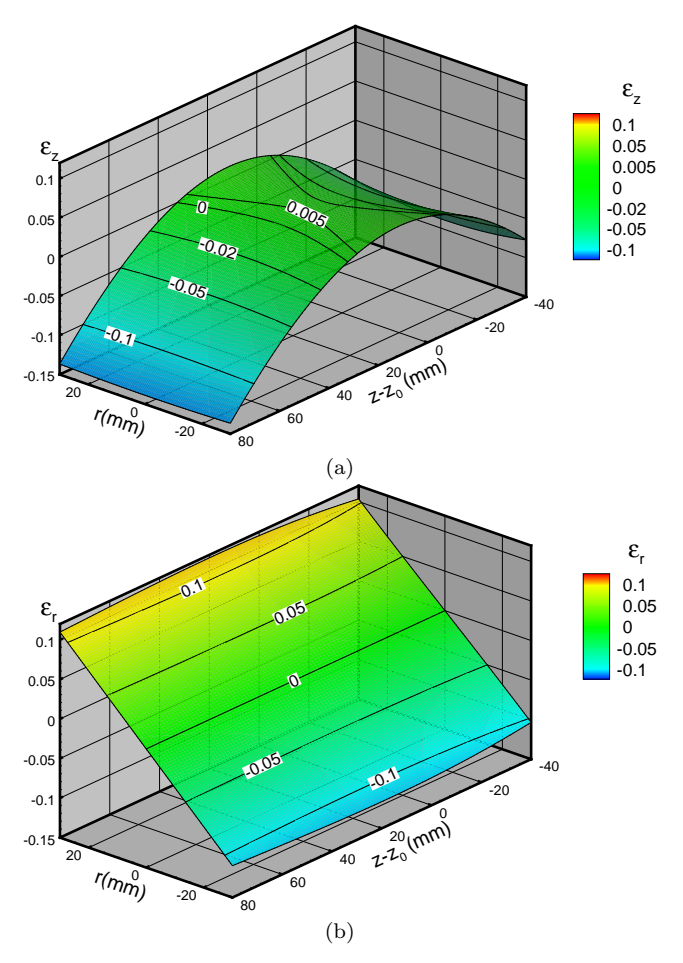


Fig. 3 Magnetic force heterogeneity axial (a) and radial (b) components for the solenoid (height: 555 mm) of the OLGA installation (Pichavant et al. 2009b). r=0,  $z=z_0=-248$  mm is one of two compensation points. Fig. 3a corresponds to the zoomed lower portion of the complete  $\nabla (B^2)_z$  curve for the OLGA solenoid (similar to that of Fig. 2).

#### 3.1 Background field heterogeneity

The spatial variation of the field heterogeneity  $\varepsilon$  can be calculated numerically when the magnetic field is known with certainty. This is the case of the magnetic field of a solenoid (Fig. 2). In Fig. 3, one can locate two compensation points at the axis (r=0) at which  $\varepsilon=0$ . One of them corresponds to the stable levitation of a bubble; another is unstable (Pichavant et al. 2009b).

Because of the cylindrical symmetry, the vector  $\varepsilon$  has only two components: axial  $\varepsilon_z$  and radial  $\varepsilon_r$ . It is important to know for the estimation purposes which field value B is necessary to obtain a given  $\varepsilon$  inside a sphere of the radius R for a substance requiring the  $|\nabla(B^2)|$  value G (see Eq. 9 and Fig. 1). The answer (Quettier et al. 2005) is given by the expression

$$B = \frac{1}{2} \sqrt{\frac{3GR}{2\varepsilon_r + \varepsilon_z}}. (11)$$

In spite of its simplicity, it gives quite accurate results. Two examples can be given for compensation in water, a case particularly important for life sciences applications. To obtain the gravity heterogeneity  $\varepsilon_z = \varepsilon_r = 1\%$  inside a sphere of 2R = 50 mm diameter, the magnetic installation should create, according to (11), the field B = 41 T. This is close to the world field record obtained with the hybrid (superconductive+resistive) installations. Such an installation would be extremely expensive. For B = 16.5 T, Eq. (11) results in  $\varepsilon = 1.2\%$  for 2R = 10 mm, which corresponds to the existing installations (Table 1).

Eq. (11) helps finding ways to improve the gravity homogeneity of an existing installation. The local B increase can be achieved by using ferromagnetic inserts inside the solenoid (Quettier et al. 2005). It is well known that the field increases in the vicinity of a ferromagnetic component. The force homogeneity calculated in presence of the insert from Fig. 4a is shown in Figs. 4b,c. The improvement of the radial heterogeneity is especially large. The calculation of the field has been performed with the Radia freeware package (Chubar et al. 1998) available from the ESRF web site together with its complete description. Comparing to the case with no insert (Figs. 3), one obtains an increase of the compensation volume by a factor 5 to 8.

## 3.2 Fluid-induced distortion of effective gravity

Let us first consider a two-phase fluid in the constant magnetic field and under Earth gravity. Since  $|\chi| \ll 1$  both for liquid and gas phases, a distortion of the background field induced by the liquid and gas domains and by the interface separating them is usually small. However, it is well known that, in the electric field, the field distortion can be strongly amplified near the regions of high interface curvature. Since the equations for the static magnetic field are similar to their electrostatic counterparts (they can also be expressed in terms of the scalar potential), an analogous effect exists in the magnetic field. The field distortion is localized in the vicinity of the high curvature interface points. We explain below that such points can appear in paramagnetic fluids like oxygen.

It is well known (Cowley and Rosensweig 1967) that the surface of a ferromagnetic fluid becomes corrugated when B exceeds a threshold value  $B_c \sim [\sigma g(\rho_L - \rho_V)]^{1/4}$ . Here  $\sigma$  is the interface tension; the indices L and V refer to liquid and vapor, respectively. The period of corrugation is  $\lambda = 2\pi l_c$ , where  $l_c = [\sigma/g(\rho_L - \rho_V)]^{1/2}$  is the capillary length. The  $\chi$  sign for paramagnetic substances is the same as for ferromagnetic substances, but the absolute value is much smaller. For this reason, the

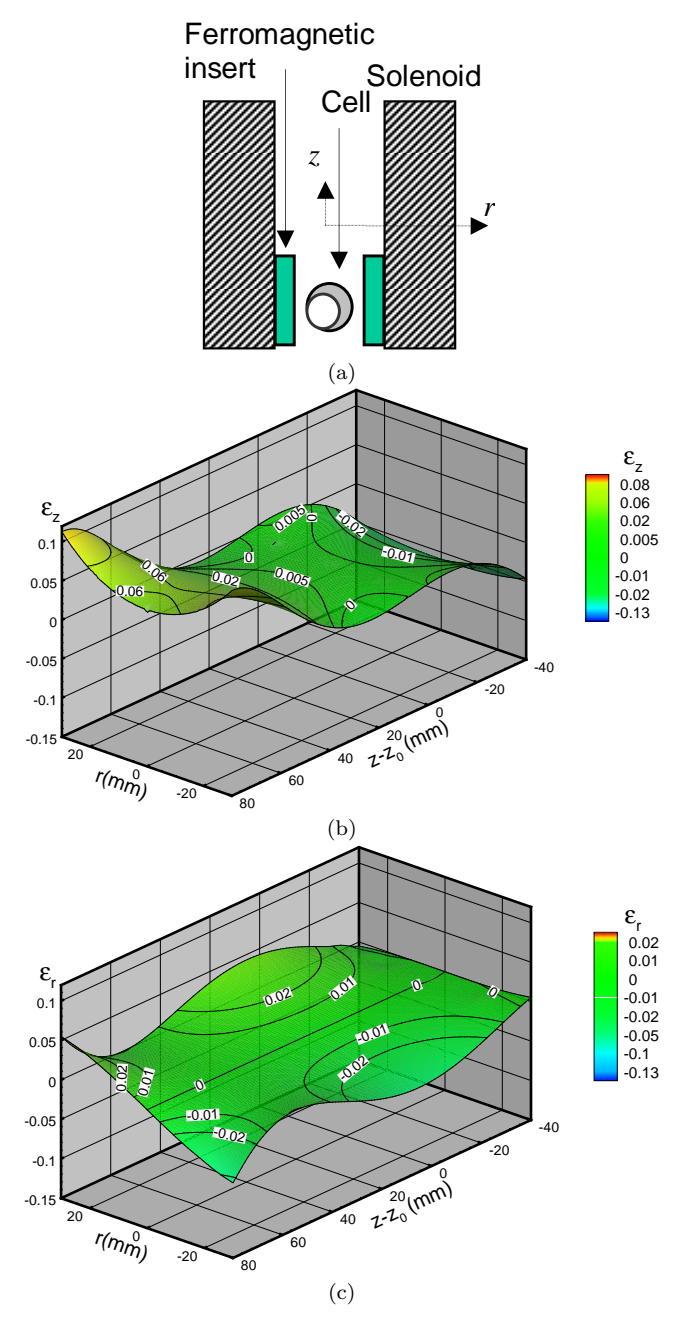
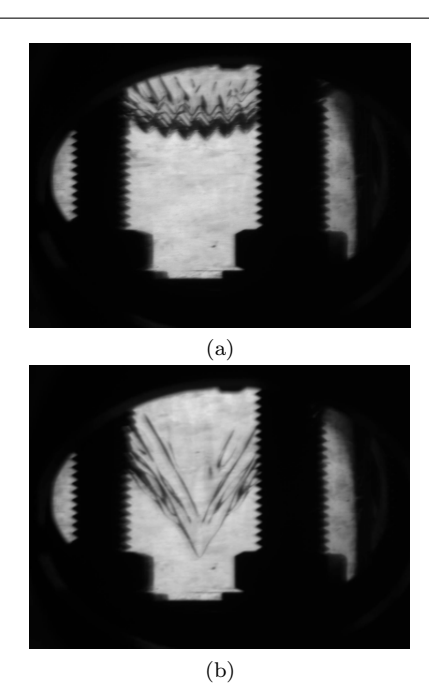


Fig. 4 Insert scheme (a). Axial (b) and radial (c) magnetic force heterogeneities for the same solenoid as that of Figs. 3 but with the insert. r = 0,  $z = z_0 = -155$  mm is the compensation point. The exact position of the insert with respect to the solenoid center is shown in Fig. 6a below.

same instability occurs for the paramagnetic fluids but at much larger fields, see Fig. 5a.

When  $\lambda/2$  is larger than the cell size, this effect leads to a distortion of the bubble shape. At some conditions it may develop a conical end (or cusp) (Takeda and Nishigaki 1994), see Fig. 5b. This means that the field is distorted in the vicinity of this end. It is the mutual amplification of the field distortion and interface defor-



**Fig. 5** Surface corrugation (a) and conical bubble shape (b) for oxygen at  $T=154.5\mathrm{K}$ , close to its critical point ( $T_c=154.8\mathrm{K}$ ,  $p_c=50$  bar) in OLGA. Two vertical threaded rods that keep the cell together are visible. Both B and  $|\nabla(B^2)|$  values for the case (b) are slightly larger than for (a).

mation that leads to the cusp geometrical singularity (Stone et al. 1999). This effect is absent in diamagnetic fluids where an interface deformation induces the field change that causes the interface smoothing.

When the field with a strong gradient is applied, the situation becomes even more complicated. It is now the effective gravity acceleration  $a_{eff}$  that needs to be used instead of g for the calculation of  $B_c$  and  $\lambda$ . Thus  $B_c \to 0$  at compensation conditions (Catherall et al. 2003) so that the instability always occurs at compensation. Since  $\lambda \to \infty$ , the interface corrugation is not observed. According to our observations, the instability manifests itself by the bubble shape deformation. Far from the critical point, bubble is of elongated oval shape. Since the instability strength is controlled by the difference  $(B-B_c)$ , the elongation should grow with B. This leads to an apparent paradox that appears when one uses a ferromagnetic insert to improve the homogeneity of the background force field (sec. 3.1). One might expect an improvement of the bubble sphericity. On the contrary, the bubble deformation grows because the insert increases B and thus strengthens the instability. Close to the critical point, a cusp appears (Fig. 5b) because the instability becomes especially strong with the decrease of  $B_c \sim [\sigma(\rho_L - \rho_V)]^{1/4}$ .

As mentioned above, this instability is absent in diamagnetic fluids.

## 3.3 Container-induced distortion of effective gravity

One needs to be particularly cautious about the materials used for the fabrication of the experimental cell and its fixation. In practice, the stainless steel is often used because of its strength and high chemical resistance to corrosion. It is considered to be a non-ferromagnetic material. This is true for a raw piece of stainless steel. Any mechanical or thermal stress converts at least some superficial layer, adjacent to the treated surface, to the ferromagnetic state. As an example, one can mention the welding joints. However, the magnetic strength (i.e. the saturation field) of such components is rather weak. Such a conversion can be easily demonstrated e.g. with a small but strong rare earth magnet.

To estimate the influence of the weakly ferromagnetic structural elements on the effective gravity field, another field heterogeneity calculation was necessary. Several cell components (Fig. 6a) with a saturation field of 0.1 T (exaggerated for estimation purposes) has been simulated. One can see that there is practically no long range force field distortion. It is limited to several mm range around the element. This means that one can use such elements provided that they are far enough from the working region. It is better however to avoid the potentially ferromagnetic materials; we replaced stainless steel by brass or titanium wherever possible.

The influence of one of the simulated elements, a flat stainless steel ring (the smallest of the three rings shown in Fig. 6a) situated at the bottom of the experimental cell was found experimentally. The vapor bubble was attracted to the ring if the distance between them was small enough. This attraction corresponds to the negative  $\varepsilon_z$  (Fig. 6b) in the vicinity of the ring, at  $z - z_0 \in [0, 5]$  mm.

## 3.4 Experimental measurement of $\varepsilon$

The experimental measurement of  $\varepsilon$  is desirable under the compensation conditions. The background force field testing is possible using a container filled with the liquid and vapor phases of the same substance. Let container be placed into the magnetic field in such a way that the bubble does not touch the container walls. Under the ideal (space) weightlessness conditions, the shape of the bubble would be spherical. Under magnetic compensation, the bubble center is situated at the compensation point or close to it. Because of the spatial variation of the magnetic force, the bubble becomes elongated (Fig. 7). From the bubble image, one can measure the bubble surface curvatures  $K_H$  and  $K_C$  at the points H and C respectively. The heterogeneity of

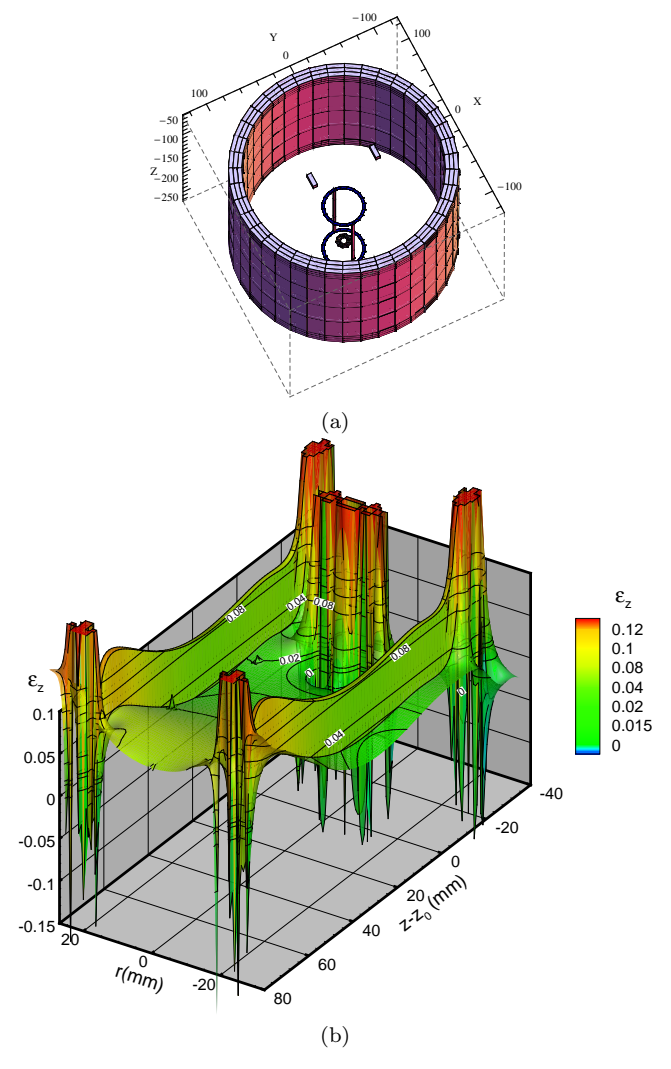


Fig. 6 (a) Several stainless steel cell components inside the OLGA ferromagnetic insert. The position of the insert with respect to the solenoid center (Fig. 4a) is shown with the coordinates in mm. The RADIA grid used for numerical calculations is visible on the insert. (b) The axial gravity heterogeneity corresponding to the geometry shown in Fig. 6a, to be compared with Fig. 4b.

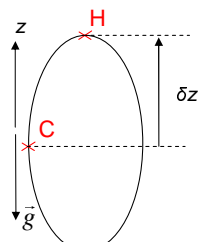


Fig. 7 Sketch of a vapor bubble magnetically levitated inside the liquid. The bubble is deformed by the residual effective gravity field.

the effective gravity acceleration can be estimated (see Appendix A) with the expression that follows from (17),

$$\varepsilon \approx l_c^2 \frac{K_H - K_C}{\delta z}.\tag{12}$$

Since  $\varepsilon_r$  is neglected in such an estimation, its accuracy is the best for small bubbles. Note that the sensitivity of this method increases with the decrease of the surface tension. For large  $\sigma$ , the bubble remains spherical even at large gravity heterogeneity and it is difficult to measure the difference of  $K_H$  and  $K_C$ .

More detailed information on the field configuration is obtained if the temperature and pressure of the fluid can be kept very close to the fluid's liquid-gas critical point (which requires, in general, a precise thermal regulation). In this case the surface tension can be made extremely small and the corresponding term can be neglected in (15). The liquid-vapor interface then follows an equipotential surface for the "magnetogravitational" potential (Lorin et al. 2009),

$$U = \frac{\alpha}{2\mu_0 g} B^2 - z. \tag{13}$$

An equipotential surface (or rather its intersection with the image plane) can thus be visualized directly (Lorin et al. 2009). Different equipotential surfaces are obtained by varying the field or the cell position. The spatial distribution of the gravity heterogeneity can be found from the shape of the equipotential lines as  $\varepsilon = \nabla U$ . The latter equation can be established by comparison of (13) with (10).

Note that the above described methods are not applicable to the case of paramagnetic fluids (sec. 3.2), where the interface deformation and magnetic field distortion are coupled and lead to a strong self-induced interface deformation even in highly homogeneous effective gravity field.

## 4 Concluding remarks

Magnetic gravity compensation method presents a powerful alternative to the classical low-gravity experimentation methods involving fluids. It becomes increasingly popular last years, especially for life sciences applications. About ten installations are available worldwide. The residual gravity heterogeneity imposes limitations on the applicability of magnetic gravity compensation. The homogeneity of the effective gravity is related to the magnetic field intensity and can be improved with ferromagnetic inserts. We propose an original method of measurement of the residual gravity from the bubble shape.

The gravity heterogeneity depends not only on the installation, but also on the sample composition and

structural elements. To reduce the gravity heterogeneity, compounds containing the ferromagnetic substances (Fe, Co, Ni, etc.) need to be avoided. The heterogeneity is the smallest for single component samples and needs to be carefully evaluated for multicomponent systems (e.g. for life sciences applications) using the magnetic susceptibility data for each of the components.

For paramagnetic substances like oxygen, an additional cause of gravity heterogeneity appears because of the coupling of the magnetic field and deformation of the gas-liquid interfaces. In this case, the effective residual gravity is more difficult to evaluate because it depends on the interface shape.

**Acknowledgements** The partial financial support by CNES and Air Liquide is gratefully acknowledged.

# Appendix A: Estimation of the effective gravity acceleration from the shape of a bubble

The shape of a vapor bubble is determined from an equation that defines a difference of pressures of vapor and liquid across the interface (Weilert et al. 1996; Chatain and Nikolayev 2002)

$$\Delta p = K\sigma + \frac{(\chi_L - \chi_V)}{2\mu_0}B^2 - (\rho_L - \rho_V)gz, \tag{14}$$

where K is the interface curvature that varies along the interface. Note that the curvature at a given point of the interface can be measured from its image. At equilibrium,  $\Delta p$  is constant along the interface. By using (4), Eq. 14 becomes

$$\Delta p = K\sigma + (\rho_L - \rho_V) \left( \frac{\alpha}{2\mu_0} B^2 - gz \right). \tag{15}$$

Let us write this equation for two arbitrary points of the bubble interface and subtract them. By denoting the difference of a quantity between these points by  $\delta$ , one obtains, by using (10),

$$\sigma \delta K = (\rho_L - \rho_V) \left( g \delta z - \frac{\alpha}{2\mu_0} \delta(B^2) \right) \approx (\rho_L - \rho_V) \, \delta z \, \, a_{eff,z}. (16)$$

Finally, one gets the estimation

$$a_{eff,z} \approx \frac{\delta K}{\delta z} \frac{\sigma}{(\rho_L - \rho_V)}.$$
 (17)

#### References

Babbick, M., Dijkstra, C., Larkin, O., Anthony, P., Davey, M., Power, J., Lowe, K., Cogoli-Greuter, M., Hampp, R.: Expression of transcription factors after short-term exposure of Arabidopsis thaliana cell cultures to hypergravity and simulated microgravity (2-D/3-D clinorotation, magnetic levitation). Adv. Space Res. 39(7), 1182 – 1189 (2007)

Ball, P.: Superconducting boost for goldfish. Nature **123**, 347 (1990)

Beaugnon, E., Tournier, R.: Levitation of water and organic substances in high static magnetic fields. J. Phys. III France 1(8), 1423 – 1428 (1991)

Beysens, D., Chatain, D., Evesque, P., Garrabos, Y.: Dynamics of phase transition in H<sub>2</sub> under high frequency vibrations. Microgravity Sci. Techn. **16**(1), 274 – 279 (2005a)

- Beysens, D., Chatain, D., Evesque, P., Garrabos, Y.: High-frequency driven capillary flows speed up the gas-liquid phase transition in zero-gravity conditions. Phys. Rev. Lett. **95**(3), 034502 (2005b)
- Beysens, D., Chatain, D., Evesque, P., Garrabos, Y.: Nucleation and growth of a bubble pattern under vibrations in weightlessness. Europhys. Lett. **82**(3), 36003 (2008)
- Beysens, D., Chatain, D., Garrabos, Y., Lecoutre, C., Palencia, F., Evesque, P., Nikolayev, V.: The effect of vibrations on heterogeneous fluids: Some studies in weightlessness. Acta Astronautica 61(11-12), 1002 – 1009 (2007)
- Beysens, D., Pichavant, G., Chatain, D., Nikolayev, V.: Phase change induced motion of  $\rm H_2$  vapour bubbles under a temperature gradient. In: ELGRA Symposium. Bonn, 1-4/09/2009~(2009)
- Braunbek, W.: Freies schweben diamagnetischer körper im magnetfeld. Z. Phys.  ${\bf 112}(11),\,764-769$  (1939)
- Brooks, J.S., Cothern, J.A.: Diamagnetism and magnetic force: a new laboratory for granular materials and chaotic/deterministic dynamics. Physica B 294 - 295, 721 - 728 (2001)
- Catherall, A.T., Benedict, K.A., King, P.J., Eaves, L.: Surface instabilities on liquid oxygen in an inhomogeneous magnetic field. Phys. Rev. E 68(3), 037302 (2003)
- Chatain, D., Nikolayev, V.S.: Using magnetic levitation to produce cryogenic targets for inertial fusion energy: experiment and theory. Cryogenics 42, 253 261 (2002)
- Chubar, O., Elleaume, P., Chavanne, J.: A three-dimensional magnetostatics computer code for insertion devices. J. Synchrotron Radiation 5(3), 481 – 484 (1998)
- Coleman, C.B., Gonzalez-Villalobos, R.A., Allen, P.L., Johanson, K., Guevorkian, K., Valles, J.M., Hammond, T.G.: Diamagnetic levitation changes growth, cell cycle, and gene expression of Saccharomyces cerevisiae. Biotechnol. Bioeng. 98(4), 854 – 863 (2007)
- Cowley, M.D., Rosensweig, R.E.: The interfacial stability of a ferromagnetic fluid. J. Fluid Mech. 30(4), 671 – 688 (1967)
- Guevorkian, K., Valles Jr, J.M.: Varying the effective buoyancy of cells using magnetic force. Appl. Phys. Lett. 84(24), 4863 – 4865 (2004)
- Hammer, B., Kidder, L., Williams, P., Xu, W.: Magnetic levitation of MC3T3 Osteoblast cells as a ground-based simulation of microgravity. Microgravity Sci. Technol. 21(4), 311 318 (2009)
- Hill, R.J.A., Eaves, L.: Nonaxisymmetric shapes of a magnetically levitated and spinning water droplet. Phys. Rev. Lett. 101(23), 234501 (2008)
- Khaldi, F., Messadek, K., Benselama, A.: Isolation of gravity effects on diffusion flames by magnetic field. Microgravity Sci. Technol. 22(1), 1-5 (2010)
- Kirichenko, Y.A., Verkin, B.I.: Simulation of zero and reduced gravity fields for heat transfer investigations under boiling. Dopovidi AN UkSSR ser. A(7), 637 640 (1968). (in Ukrainian)
- Kiyoshi, T., Wada, H.: Development of advanced high-field magnets at the Tsukuba magnet laboratory. J. Low Temp. Phys. 133(1), 31 40 (2003)
- Liu, Y., Zhu, D.M., Strayer, D.M., Israelsson, U.E.: Magnetic levitation of large water droplets and mice. Adv. Space Res. 45(1), 208 – 213 (2010)
- Lorin, C., Mailfert, A., Chatain, D., Félice, H., Beysens, D.: Magnetogravitational potential revealed near a liquid-vapor critical point. J. Appl. Phys. 106(3), 033905 (2009)
- Lu, H.M., Yin, D.C., Li, H.S., Geng, L.Q., Zhang, C.Y., Lu, Q.Q., Guo, Y.Z., Guo, W.H., Shang, P., Wakayama, N.I.: A containerless levitation setup for liquid processing in a supercontainer.

- ducting magnet. Rev. Sci. Instrum. 79(9), 093903 (2008)
- Lyon, D.N., Jones, M.C., Ritter, G.L., Chiladakis, C.I., Kosky, P.G.: Peak nucleate boiling fluxes for liquid oxygen on a flat horizontal platinum surface at buoyancies corresponding to accelerations between -0.03 and 1g<sub>E</sub>. AIChE J. 11(5), 773 – 780 (1965)
- Lyuksyutov, I.F., Naugle, D.G., Rathnayaka, K.D.D.: On-chip manipulation of levitated femtodroplets. Appl. Phys. Lett. **85**(10), 1817 1819 (2004)
- Manzano, A., Matía, I., González-Camacho, F., Carnero-Díaz, E., van Loon, J., Dijkstra, C., Larkin, O., Anthony, P., Davey, M., Marco, R., Medina, F.: Germination of Arabidopsis seed in space and in simulated microgravity: Alterations in root cell growth and proliferation. Microgravity Sci. Technol. 21(4), 293 297 (2009a)
- Manzano, A.I., Dijkstra, C., Larkin, O., Anthony, P., Davey, M.R., Hill, R.J., Eaves, L., Carnero-Díaz, E., Medina, F.J.: Expression of cyclin B1 gene, a cell cycle regulator, is enhanced in young Arabidopsis seedlings grown in altered gravity, under magnetic levitation. In: ELGRA Symposium. Bonn, 1-4/09/2009 (2009b)
- Manzano, A.I., Dijkstra, C., Larkin, O., Anthony, P., Davey, M.R., Hill, R.J., Eaves, L., Carnero-Díaz, E., Medina, F.J.: A sequential study on early plant development under magnetic levitation shows effects of altered gravity on cell proliferation and growth. In: ELGRA Symposium. Bonn, 1-4/09/2009 (2009c)
- Matsumoto, S., Kiyoshi, T., Asano, T., Sato, A., Wada, H.: Comprehensive applications of high magnetic fields at TML. Physica B **346 347**, 633 637 (2004). Proceedings of the 7th International Symposium on Research in High Magnetic Fields.
- Moes, M., Gielen, J., Bleichrodt, R., van Loon, J., Christianen, P., Boonstra, J.: Magnetic levitation of human A431 cells. In: ELGRA Symposium. Bonn, 1-4/09/2009 (2009)
- Nikolayev, V.S., Chatain, D., Garrabos, Y., Beysens, D.: Experimental evidence of the vapor recoil mechanism in the boiling crisis. Phys. Rev. Lett. 97, 184503 (2006)
- Pichavant, G., Beysens, D., Chatain, D., Communal, D., Lorin, C., Mailfert, A.: Using superconducting magnet to reproduce quick variations of gravity in liquid oxygen. In: ELGRA Symposium. Bonn, 1-4/09/2009 (2009a)
- Pichavant, G., Cariteau, B., Chatain, D., Beysens, D., Nikolayev, V.S., Communal, D., Bonnay, P.: Magnetic gravity compensation setup to create variable gravity levels and fast transients in O<sub>2</sub> (2010). Submitted to: Rev. Sci. Instr.
- Pichavant, G., Cariteau, B., Chatain, D., Nikolayev, V., Beysens, D.: Magnetic compensation of gravity: Experiments with oxygen. Microgravity Sci. Techn. 21(1), 129 – 133 (2009b)
- Quettier, L., Félice, H., Mailfert, A., Chatain, D., Beysens, D.: Magnetic compensation of gravity forces in liquid/gas mixtures: surpassing intrinsic limitations of a superconducting magnet by using ferromagnetic inserts. Eur. Phys. J. Appl. Phys. 32(3), 167 – 175 (2005)
- Simon, M.D., Geim, A.K.: Diamagnetic levitation: Flying frogs and floating magnets. J. Appl. Phys. **87**(9), 6200 6204 (2000)
- Stone, H.A., Lister, J.R., Brenner, M.P.: Drops with conical ends in electric and magnetic fields. Proc. R. Soc. Lond. A 455, 329 – 347 (1999)
- Sueda, M., Katsuki, A., Nonomura, M., Kobayashi, R., Tanimoto, Y.: Effects of high magnetic field on water surface phenomena. J. Phys. Chem. C 111(39), 14389 – 14393 (2007)
- Tagami, M., Hamai, M., Mogi, I., Watanabe, K., Motokawa, M.: Solidification of levitating water in a gradient strong magnetic field. J. Crystal Growth 203(4), 594 – 598 (1999)

- Takeda, M., Nishigaki, K.: Deformation of the liquid oxygen meniscus induced by magnetic field. J. Phys. Soc. Japan **63**(4), 1345 1350 (1994)
- Valles Jr, J.M., Lin, K., Denegre, J.M., Mowry, K.L.: Stable magnetic field gradient levitation of Xenopus laevis: toward low-gravity simulation. Biophysical J. **73**(2), 1130 1133 (1997)
- Watanabe, K., Takahashi, K., Mogi, I., Nishijima, G., Awaji, S., Motokawa, M.: Cryogen-free hybrid magnet for magnetic levitation. Physica C 386, 485 – 489 (2003)
- Weilert, M.A., Whitaker, D.L., Maris, H.J., Seidel, G.M.: Magnetic levitation and noncoalescence of liquid helium. Phys. Rev. Lett. **77**(23), 4840 4843 (1996)
- Whitaker, D.L., Kim, C., Vicente, C.L., Weilert, M.A., Maris, H.J., Seidel, G.M.: Shape oscillations in levitated He II drops. J. Low Temp. Phys. **113**(3), 491 – 499 (1998)
- Wunenburger, R., Chatain, D., Garrabos, Y., Beysens, D.: Magnetic compensation of gravity forces in (p-) hydrogen near its critical point: Application to weightless conditions. Phys. Rev. E **62**(1), 469 476 (2000)